



HAL
open science

Quartic Parameters for Acoustic Applications of Lattice Boltzmann Scheme

François Dubois, Pierre Lallemand

► **To cite this version:**

François Dubois, Pierre Lallemand. Quartic Parameters for Acoustic Applications of Lattice Boltzmann Scheme. *Computers & Mathematics with Applications*, 2011, 61, pp.3404-3416. 10.1016/j.camwa.2011.01.011 . hal-00451274v3

HAL Id: hal-00451274

<https://hal.science/hal-00451274v3>

Submitted on 11 Jun 2011

HAL is a multi-disciplinary open access archive for the deposit and dissemination of scientific research documents, whether they are published or not. The documents may come from teaching and research institutions in France or abroad, or from public or private research centers.

L'archive ouverte pluridisciplinaire **HAL**, est destinée au dépôt et à la diffusion de documents scientifiques de niveau recherche, publiés ou non, émanant des établissements d'enseignement et de recherche français ou étrangers, des laboratoires publics ou privés.

Quartic Parameters for Acoustic Applications of Lattice Boltzmann Scheme

François Dubois ^{ab} and Pierre Lallemand ^c

^a *Conservatoire National des Arts et Métiers,
Department of Mathematics, Paris, France.*

^b *Department of Mathematics, University Paris-Sud,
Bât. 425, F-91405 Orsay Cedex, France
francois.dubois@math.u-psud.fr*

^c *Centre National de la Recherche Scientifique, Paris, France.
pierre.lallemand1@free.fr*

11 June 2011 *

Abstract. - Using the Taylor expansion method, we show that it is possible to improve the lattice Boltzmann method for acoustic applications. We derive a formal expansion of the eigenvalues of the discrete approximation and fit the parameters of the scheme to enforce fourth order accuracy. The corresponding discrete equations are solved with the help of symbolic manipulation. The solutions are obtained in the case of D3Q27 lattice Boltzmann scheme. Various numerical tests support the coherence of this approach.

Keywords: Taylor expansion method, linearized Navier–Stokes.

* Invited Presentation, Sixth International Conference for Mesoscopic Methods in Engineering and Science (ICMMES-2009), Guangzhou City (Canton), Guangdong Province, China, July 13-17, 2009. Published, *Computers And Mathematics With Applications*, volume 61, pages 3404-3416, june 2011, doi:10.1016/j.camwa.2011.01.011.

1) Introduction

- The lattice Boltzmann equation methodology is a general framework for approximating problems that are modelled by partial differential equations under conservative form arising in physics. It has been first proposed for fluid dynamics in the context of cellular automata (see *e.g.* Hardy *et al* [17], Wolfram [36], d’Humières *et al* [6]). The classical lattice Boltzmann scheme (McNamara-Zanetti [27], Higuera *et al* [20], Qian *et al* [29], d’Humières [5]) has been first developed for nonlinear fluid problems. It has also the capability to approximate thermal flows. (Chen *et al* [4]), magnetohydrodynamics (Dellar [7]) or coupling between fluid and structures (see *e.g.* Kwon [22]).

- We have proposed in [8, 9] the Taylor expansion method to analyze formally the d’Humières lattice Boltzmann scheme [5] when the mesh size tends to zero. We have then replaced the (much more) formal Chapman-Enskog expansion methodology used in [5] by a simple Taylor expansion relative to the grid spacing. In this way we can obtain the modified equations of the scheme (in the sense of Lerat-Peyret [25] and Warming-Hyett [34]; see also [16, 2, 33]) at an arbitrary order in the general nonlinear case. We made more explicit in [10] the result at third order accuracy in all generality. We have observed at this occasion that a serious difficulty with the lattice Boltzmann scheme lies in the fact that the equivalent mass conservation equation contains an *a priori* non-null third order term. We have also proposed an algorithm to derive the modified equation in the case of linearized problems [11]. We have applied this methodology to derive the so-called “quartic parameters” to enhance the accuracy of the lattice Boltzmann scheme to simulate shear waves [11]. An application of this result is used by Leriche *et al* [26] for computing with spectral method and lattice Boltzmann scheme the eigenmodes of the Stokes problem in a cube. This Taylor expansion method can also be used for a detailed analysis of boundary conditions. In [12] we have shown that the “magic boundary parameters” of Ginzburg and Adler [14] depend in fact upon the detailed choice of the parameters of the lattice Boltzmann scheme.

- In this contribution, we consider linearized athermal acoustics in two and three space dimensions. In Section 2, we recall the essential properties of the d’Humières scheme. Then in Section 3, we use the method of formal expansion to expand the discrete eigenmodes of the acoustic system of partial differential equations as the mesh size tends to zero. In Section 4, we increase the accuracy of the lattice Boltzmann scheme with the development of “quartic” parameters and develop also a weaker approach by enforcing isotropy at fourth order accuracy. Applications in two and three space dimensions (D2Q13 and D3Q27 schemes) are presented in Sections 5 and 6 respectively. We detail our version of the D3Q27 scheme and the explicit formulae for the determination of the quartic parameters.

2) d’Humières lattice Boltzmann scheme

• In the framework proposed by d’Humières [5], the lattice Boltzmann scheme uses a regular lattice \mathcal{L} with typical mesh size Δx and for each node x in \mathcal{L} , a discrete set of $(J + 1)$ velocities \mathcal{V} is given. In this contribution, the set \mathcal{V} does not depend on the vertex x . We introduce a velocity scale λ and the time step Δt is obtained according to the so-called “acoustic scaling” :

$$(1) \quad \Delta t = \frac{\Delta x}{\lambda}$$

For $x \in \mathcal{L}$ and $v_j \in \mathcal{V}$, the point $x + v_j \Delta t$ is supposed to be a new vertex of the lattice. The unknown of this lattice Boltzmann scheme is the particle distribution $f_j(x, t)$ for $x \in \mathcal{L}$, $0 \leq j \leq J$ and discrete values of time t . The numerical scheme proceeds into two major steps.

• The first step describes the relaxation $f \rightarrow f^*$ of particle distribution f towards a locally defined equilibrium. It is local in space and nonlinear in general. In this paper devoted to acoustics we consider only linear contributions. It is defined with the help of a fixed invertible matrix M . The moments m_k are defined through a simple linear relation

$$(2) \quad m_k = \sum_{j=0}^J M_{kj} f_j, \quad 0 \leq k \leq J.$$

Note that this very simple **linear** hypothesis is not satisfied in the scheme proposed by Geier *et al* [13]. The first $d + 1$ moments (where d is the space dimension, equal to $d = 2$ or $d = 3$ in the present applications) are the total density ρ and the momentum q_α :

$$(3) \quad \begin{cases} m_0 = \rho \equiv \sum_{j=0}^J f_j \\ m_\alpha = q_\alpha \equiv \sum_{j=0}^J v_j^\alpha f_j, \quad 1 \leq \alpha \leq d. \end{cases}$$

We denote by W the vector (in \mathbb{R}^N) composed of the density and the components of the momentum. These moments are supposed to be at equilibrium:

$$(4) \quad m_i^* = m_i \equiv m_i^{\text{eq}} \equiv W_i, \quad 0 \leq i \leq d.$$

The relaxation evolution $m \rightarrow m^*$ due to linearized collisions is local and trivial for the vector W of conserved quantities, as remarked in (4). For the other moments, a distribution of equilibrium moments $G(\bullet)$ is given as a (linear for the present study of acoustic waves) function of the vector W :

$$(5) \quad m_k^{\text{eq}} = G_k(W), \quad d < k \leq J.$$

For $k \geq N$, the evolution $m \rightarrow m^*$ is supposed to be uncoupled:

$$(6) \quad m_k^* = m_k + s_k (m_k^{\text{eq}} - m_k), \quad k > d.$$

It is parametrized by the so-called ‘‘relaxation rate parameters’’ s_k . For stability reasons (see *e.g.* Lallemand and Luo [23]), we have the inequalities

$$(7) \quad 0 < s_k < 2, \quad k > d.$$

When the components $m_k^*(x, t)$ are computed for each $x \in \mathcal{L}$ at discrete time t , the distribution $f_j^*(x, t)$ after relaxation is reconstructed by inversion of relation (2):

$$(8) \quad f_j^* = \sum_{\ell=0}^J M_{j\ell}^{-1} m_\ell^*, \quad 0 \leq j \leq J.$$

- The second step is just a free advective evolution without collision through characteristics:

$$(9) \quad f_j(x, t + \Delta t) = f_j^*(x - v_j \Delta t, t), \quad 0 \leq j \leq J, \quad x \in \mathcal{L}.$$

- The asymptotic analysis of cellular automata provides evidence supporting asymptotic partial differential equations with transport coefficients related to the induced parameter defined by the so-called Hénon’s relation [18]

$$(10) \quad \sigma_k \equiv \frac{1}{s_k} - \frac{1}{2}.$$

The lattice Boltzmann scheme is classically considered as second order accurate (see *e.g.* [23]). We describe in Section 6 the D3Q27 ($d = 3$, $J = 26$) numerical scheme that we used for acoustic application.

3) Formal development of eigenmodes

- With the method described in [11], it is possible to derive the equivalent system of $(d + 1)$ equations associated to a lattice Boltzmann scheme. The system of linearized conservation equations issued from this analysis can be written under the form

$$(11) \quad A(\Delta x, \partial) \bullet W = 0$$

which uses a compact notation stating that $A(\Delta x, \partial)$ is a $(d + 1) \times (d + 1)$ (4×4 for three-dimensional applications, 3×3 for two-dimensional models) matrix of differential operators of high order acting on the conserved variables W .

We seek the eigenmodes of the operator $A(\Delta x, \partial)$, *id est* the eigenvalues $\lambda_j(\Delta x, \partial)$ and the eigenvectors $r_j(\Delta x, \partial)$ such that

$$(12) \quad A(\Delta x, \partial) \bullet r_j(\Delta x, \partial) = \lambda_j(\Delta x, \partial) r_j(\Delta x, \partial), \quad 0 \leq j \leq d.$$

We introduce the diagonal matrix $\Lambda(\Delta x, \partial)$ composed of the eigenvalues $\lambda_j(\Delta x, \partial)$ and the square matrix $R(\Delta x, \partial)$ composed of the eigenvectors. Then relation (12) can be written under the following synthetic form:

$$(13) \quad A(\Delta x, \partial) \bullet R(\Delta x, \partial) = R(\Delta x, \partial) \bullet \Lambda(\Delta x, \partial).$$

• Moreover, the operator $A(\Delta x, \partial)$ in equation (11) is a formal series in the variable Δx that is truncated at order 4 in this contribution:

$$(14) \quad A(\Delta x, \partial) \equiv A_0(\partial) + \Delta x A_1(\partial) + \Delta x^2 A_2(\partial) + \Delta x^3 A_3(\partial) + O(\Delta x^4).$$

We can apply in this case the so-called stationary perturbation theory for linear operators (see *e.g.* [3] for an elementary introduction). First for $\Delta x = 0$, the operator $A_0(\partial)$ is exactly the perfect linear acoustic model. For $d = 3$ (the case $d = 2$ is a simple consequence of this particular analysis and we omit the details), we have

$$(15) \quad A_0(\partial) = \begin{pmatrix} \partial_t & \partial_x & \partial_y & \partial_z \\ c_0^2 \partial_x & \partial_t & 0 & 0 \\ c_0^2 \partial_y & 0 & \partial_t & 0 \\ c_0^2 \partial_z & 0 & 0 & \partial_t \end{pmatrix}.$$

Introducing the Laplacian operator $\Delta \equiv \partial_x^2 + \partial_y^2 + \partial_z^2$, a system $R_0(\partial)$ of reference eigenvectors can be given under the form

$$(16) \quad R_0(\partial) = \begin{pmatrix} c_0 \sqrt{\Delta} & -c_0 \sqrt{\Delta} & 0 & 0 \\ c_0^2 \partial_x & c_0^2 \partial_x & \partial_y & -\partial_{xz}^2 \\ c_0^2 \partial_y & c_0^2 \partial_y & -\partial_x & -\partial_{yz}^2 \\ c_0^2 \partial_z & c_0^2 \partial_z & 0 & \partial_x^2 + \partial_y^2 \end{pmatrix}.$$

It is elementary to observe the relation

$$(17) \quad A_0(\partial) \bullet R_0(\partial) = R_0(\partial) \bullet \Lambda_0(\partial)$$

and the associated matrix $\Lambda_0(\partial)$ of order zero is simply given by

$$(18) \quad \Lambda_0(\partial) = \begin{pmatrix} \partial_t + c_0 \sqrt{\Delta} & 0 & 0 & 0 \\ 0 & \partial_t - c_0 \sqrt{\Delta} & 0 & 0 \\ 0 & 0 & \partial_t & 0 \\ 0 & 0 & 0 & \partial_t \end{pmatrix}.$$

We observe that even if the eigenvalue ∂_t is degenerated, *i.e.* when the eigenvalues are multiple, the family of eigenvectors proposed in (16) is complete and defines a basis. This allows us to show the existence of two acoustic waves and two shear waves (see *e.g.* [24]).

- The parameter Δx is supposed to be infinitesimal and we introduce a formal expansion of the eigenvalues with **diagonal** matrices $\Lambda_j(\partial)$:

$$(19) \quad \Lambda(\Delta x, \partial) \equiv \Lambda_0(\partial) + \Delta x \Lambda_1(\partial) + \Delta x^2 \Lambda_2(\partial) + \Delta x^3 \Lambda_3(\partial) + O(\Delta x^4)$$

and relative perturbations $Q_j(\partial)$ of the eigenvectors:

$$(20) \quad R(\Delta x, \partial) \equiv R_0(\partial) \bullet (\text{Id} + \Delta x Q_1(\partial) + \Delta x^2 Q_2(\partial) + \Delta x^3 Q_3(\partial) + O(\Delta x^4)).$$

We adopt in this work the scaling condition for eigenvectors proposed *e.g.* by Cohen-Tannoudji *et al* [3]. The component of $r_j(\Delta x, \partial)$ relative to the corresponding unperturbed eigenvector is exactly equal to unity. In other words, all the diagonal terms of the $Q_j(\partial)$ matrices are null:

$$(21) \quad Q_j(\partial)_{\ell\ell} = 0, \quad 0 \leq \ell \leq d, \quad j \geq 1.$$

We insert the expansions (20) and (21) into the eigenmode condition (13). We introduce the expression $\tilde{A}_j(\partial)$ for the perturbation relative to the unperturbed eigenbasis, *id est*

$$(22) \quad \tilde{A}_j(\partial) \equiv R_0(\partial)^{-1} \bullet A_j(\partial) \bullet R_0(\partial).$$

Then we identify each term relative to Δx and we obtain in this manner:

$$(23) \quad \Lambda_1(\partial) \equiv \tilde{A}_1(\partial) + \Lambda_0(\partial) \bullet Q_1(\partial) - Q_1(\partial) \bullet \Lambda_0(\partial)$$

$$(24) \quad \Lambda_2(\partial) \equiv \tilde{A}_2(\partial) + \tilde{A}_1(\partial) \bullet Q_1(\partial) - Q_1(\partial) \bullet \Lambda_1(\partial) + \Lambda_0(\partial) \bullet Q_2(\partial) - Q_2(\partial) \bullet \Lambda_0(\partial)$$

$$(25) \quad \Lambda_3(\partial) \equiv \begin{cases} \tilde{A}_3(\partial) + \tilde{A}_2(\partial) \bullet Q_1(\partial) - Q_1(\partial) \bullet \Lambda_2(\partial) \\ + \tilde{A}_1(\partial) \bullet Q_2(\partial) - Q_2(\partial) \bullet \Lambda_1(\partial) \\ + \Lambda_0(\partial) \bullet Q_3(\partial) - Q_3(\partial) \bullet \Lambda_0(\partial) \end{cases}.$$

Explicit forms of the eigenvalues at each order may be found without difficulty using symbolic manipulation.

- We introduce a reference density ρ_0 , a reference sound velocity c_0 , the shear viscosity μ and the bulk viscosity ζ . It is well known (see *e.g.* Landau-Lifshitz [24]) that the four compressible isothermal acoustic linearized equations take the form:

$$(26) \quad \begin{cases} \partial_t \rho + \rho_0 \operatorname{div} \mathbf{u} = 0 \\ \rho_0 \partial_t u + c_0^2 \partial_x \rho - \mu \Delta u - \left(\zeta + \frac{\mu}{3} \right) \partial_x (\operatorname{div} \mathbf{u}) = 0 \\ \rho_0 \partial_t v + c_0^2 \partial_y \rho - \mu \Delta v - \left(\zeta + \frac{\mu}{3} \right) \partial_y (\operatorname{div} \mathbf{u}) = 0 \\ \rho_0 \partial_t w + c_0^2 \partial_z \rho - \mu \Delta w - \left(\zeta + \frac{\mu}{3} \right) \partial_z (\operatorname{div} \mathbf{u}) = 0 \end{cases}$$

with $\operatorname{div} \mathbf{u} \equiv \partial_x u + \partial_y v + \partial_z w$ and we recognize matrix (15) when $\mu = \zeta = 0$. This system has two families of eigenvalues.

- On the one hand, the acoustic waves λ_{\pm} are given by

$$(27) \quad \lambda_{\pm} = \partial_t - \gamma \Delta \pm c_0 \sqrt{\Delta} \sqrt{1 + \frac{\gamma^2}{c_0^2} \Delta}$$

and are parametrized by the attenuation of the sound waves γ given according to

$$(28) \quad \gamma = \frac{1}{2\rho_0} \left(\zeta + \frac{d+1}{d} \mu \right).$$

We can expand the previous acoustic wave eigenvalues in powers of γ when the attenuation is sufficiently small compared to the frequency of the sound waves. Then we have the expansion

$$(29) \quad \lambda_{\pm} = \partial_t \pm c_0 \sqrt{\Delta} - \gamma \Delta \pm \frac{1}{2} \frac{\gamma^2}{c_0} \Delta^{3/2} + \mathcal{O}(\gamma^4).$$

The previous (relatively unusual) notations with matrices of operators are **exactly the one used** when implementing without difficulty (due to linearity) our approach with a symbolic manipulation software. As is well known, the pseudo-differential operators like $\sqrt{\Delta}$ and $\Delta^{3/2}$ are defined by their action on Fourier transforms (we refer *e.g.* to the book of Hörmander [21]). It is also possible to introduce a Fourier decomposition on harmonic waves of the type $\exp(i(\omega t - \mathbf{k} \cdot \mathbf{x}))$. Then we have the usual change of notation: $\partial_t \equiv i\omega$, $\nabla \equiv -i\mathbf{k}$, $\Delta \equiv -|\mathbf{k}|^2$, $\Delta^{3/2} \equiv -i|\mathbf{k}|^3$, *etc.* The corresponding dispersion relation associated with the annulation of the eigenvalues λ_{\pm} given in (29) allows the introduction of the parameter Γ_{ℓ} according to

$$(30) \quad -i\omega \equiv \Gamma_{\ell} = \gamma |\mathbf{k}|^2 \pm i c_0 |\mathbf{k}| \left(1 - \frac{\gamma^2}{2c_0^2} |\mathbf{k}|^2 \right) + \mathcal{O}(\gamma^4 |\mathbf{k}|^5).$$

- On the other hand, the shear wave λ_0 define a multiple eigenmode that is simply given by

$$(31) \quad \lambda_0 = \partial_t - \nu \Delta$$

with $\nu \equiv \frac{\mu}{\rho_0}$. With the spectral notation, relation (31) can be written with the help of the attenuation Γ_t of the shear waves under the form

$$(32) \quad -i\omega \equiv \Gamma_t = \nu |\mathbf{k}|^2 .$$

As previously, a family of **two** independent eigenvectors with two different ‘‘polarizations’’ corresponds to this shear eigenvalue. Moreover, the perturbation $\Delta x A_1(\partial) + \Delta x^2 A_2(\partial) + \Delta x^3 A_3(\partial) + \dots$ of relation (14) is **diagonal** on the basis of unperturbed eigenvectors proposed at relation (16). Due to well-established arguments (see *e.g.* the textbook of Quantum Mechanics of Cohen-Tannoudji *et al* [3] or *e.g.* the sections ‘‘multiple roots’’ and ‘‘degenerate roots’’ in the book of Hinch [19]), the expansion (20) (21) is completely valid even in this (relatively) complicated degenerate case.

4) Increasing the accuracy of shear and acoustic waves

- When we use a lattice Boltzmann scheme, the viscosity μ admits a representation of the type (*c.f.* the D3Q27 scheme):

$$(33) \quad \mu = \frac{1}{3} \lambda \Delta x \sigma_x$$

and similarly the bulk viscosity ζ is given for the D3Q27 scheme (to fix the ideas) according to

$$(34) \quad \zeta = \lambda \Delta x \sigma_e \left(\frac{5}{9} - c_0^2 \right)$$

with the notations of Section 6. We can identify the developments (19) on the one hand and (29)(31) on the other hand because, due to (33), (34) and (28), the viscosities γ and μ are proportional to Δx . The usual implementation of lattice Boltzmann scheme consists in adjusting the eigenvalues $\Lambda_0(\partial)$ and $\Lambda_1(\partial)$ in order to fit the viscosities.

- When we identify the developments (19) and (31) at the order 4 for the shear waves, we recover the ‘‘quartic parameters’’ obtained previously [11], in particular for the D2Q9 [23] and D3Q19 [32] schemes. In these cases, the shear viscosity μ follows the ‘‘quartic’’ condition

$$(35) \quad \mu = \frac{1}{\sqrt{108}} \lambda \Delta x .$$

If we add to the previous study the fitting of the acoustic waves (29), there is no solution of the equations for the two previous schemes D2Q9 and D3Q19. We have then considered the previous conditions for extended stencils such as the D2Q13 [30, 35] and D3Q27 (see *e.g.* [28]) lattice Boltzmann schemes. The results for quartic coefficients are displayed in Section 6 when fitting all the waves (29) and (31) of the linear problem.

- In order to take advantage of the flexibility of the d’Humières scheme, we have developed an “isotropic” condition, not as strong as the quartic condition. With this isotropic condition, we do not impose anymore the conditions that the numerical waves (19) fit exactly the physical ones (29) and (31) but suggest that the numerical waves are isotropic. In other words, the operator matrices $\Lambda_2(\partial)$ (for the order 3) and $\Lambda_3(\partial)$ (for the order 4) are differential operators that are constrained in order to depend only on the radial variable r ($r^2 \equiv x^2 + y^2 + z^2$) and on the operator $\partial/\partial r$. When this condition is imposed, it is possible to fit isotropic waves for the four previous schemes. In Table 1 and 2, we display the number of (*a priori* non-independent) discrete equations that must be satisfied by the parameters of the lattice Boltzmann schemes when we impose isotropy for the shear waves, isotropy for the acoustic waves, exact fitting of the shear waves and exact fitting of the acoustic waves. All these discrete equations have been solved exactly with the help of symbolic manipulation. To fix the ideas, we give in Section 6 the parametrization of the quartic shear and acoustic waves for the D3Q27 lattice Boltzmann scheme (solution of 18 discrete equations, according to Table 2).

	isotropic shear	isotropic acoustic	exact shear	exact acoustic
order 3	0	1	0	2
order 4	1	1	2	2

Table 1. *Fitting “isotropic” and “exact” shear and acoustic waves at various orders of accuracy. Number of equations for the D2Q9 and D2Q13 lattice Boltzmann schemes. Note that the same numbers apply to both lattices.*

	isotropic shear	isotropic acoustic	exact shear	exact acoustic
order 3	0	1	0	2
order 4	10	2	13	3

Table 2. *Fitting “isotropic” and “exact” shear and acoustic waves at various orders of accuracy. Number of equations for the D3Q19 and D3Q27 lattice Boltzmann schemes. Note that the same numbers apply to both lattices.*

5) Linearized acoustics with the D2Q13 scheme

- Two numerical “experiments” have been performed: emission from the center (Figures 1, 2 and 3) and emission from the boundary of the circle (see Figures 1, 4, 5, 6). In both cases, a first order anti-bounce-back boundary condition (see *e.g.* [1]) is implemented to impose a given density (pressure) on the boundary: either a constant when sound is emitted at the center, or a sinusoidal time dependent value for the emission by the boundary. In each case, we measure the value of the density at a fixed position in space *vs* time (see Figure 6) or we analyze the pressure field at a given time (see Figures 2 to 5). Obviously the maximum duration of the simulation with a radius R and sound velocity c_0 is R/c_0 when the source is at the center and $2R/c_0$ when it is on the circular boundary. These experiments are sensitive to anisotropic behaviour of both the velocity and of the attenuation as can be seen in the figures.

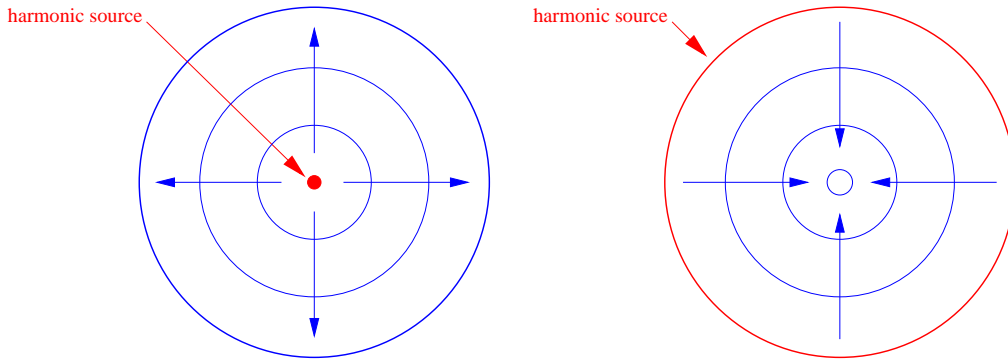


Figure 1. *Diverging (left) and converging (right) acoustic test cases.*

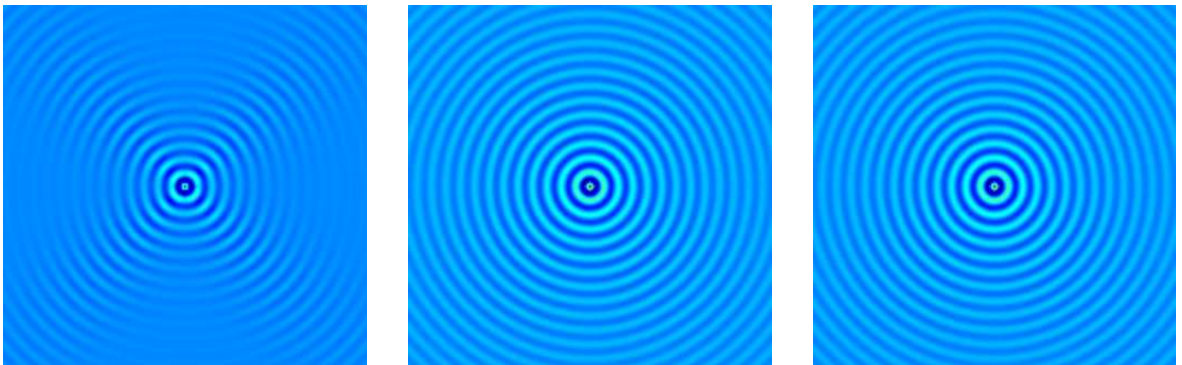


Figure 2. *D2Q13 Acoustic propagation, diverging acoustic test case, time period = 8 (7 points per wave length, $c_0^2 = 0.80$): usual (left), isotropic (center) and quartic (right).*

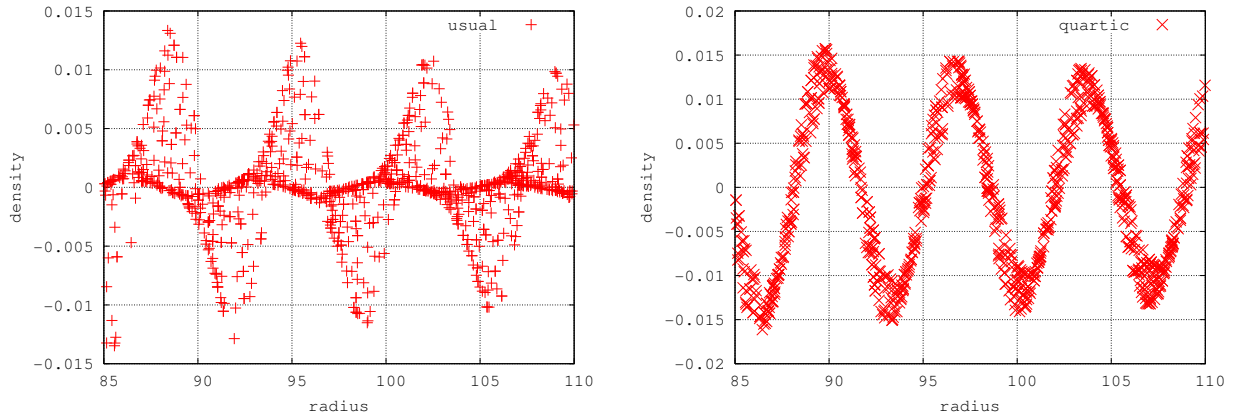


Figure 3. *D2Q13 diverging acoustic test case. Measurements after 200 time steps; usual parameters (left) and quartic parameters (right).*

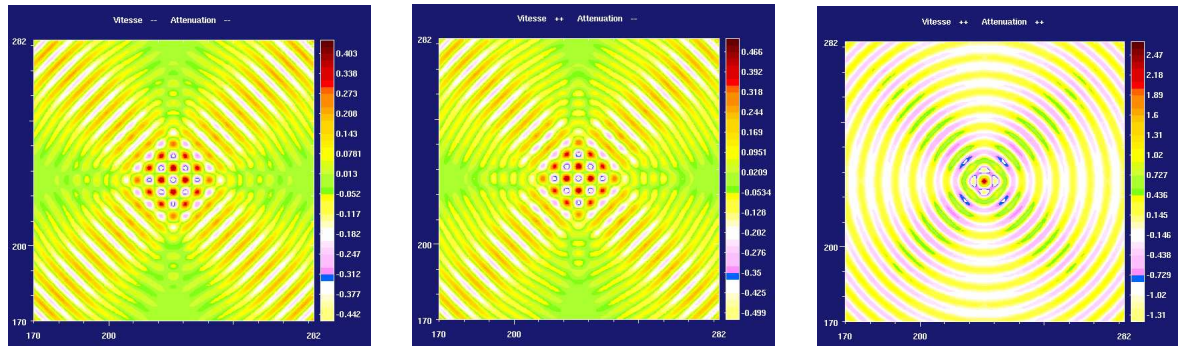


Figure 4. *D2Q13 Converging acoustic propagation, time period = 8 (7 points per wave length, $c_0^2 = 0.80$): usual (left), isotropic (center) and quartic (right).*

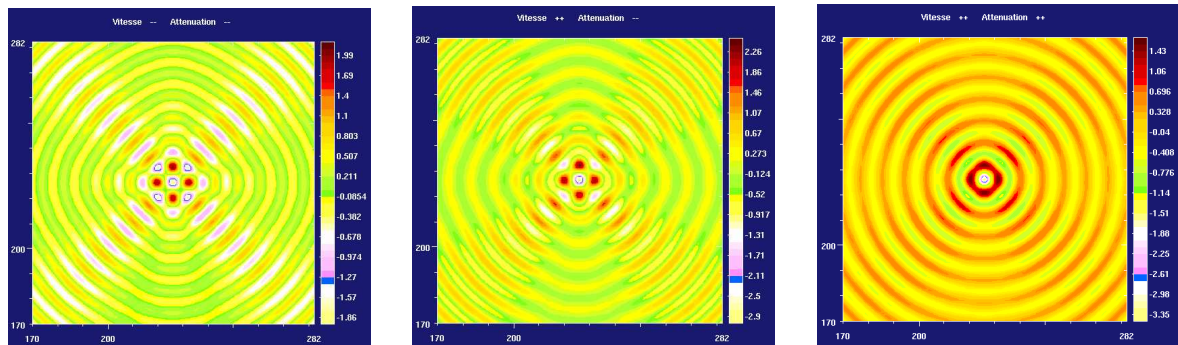


Figure 5. *D2Q13 Converging acoustic propagation, time period = 10 (9 points per wave length, $c_0^2 = 0.80$): usual (left), isotropic (center) and quartic (right).*

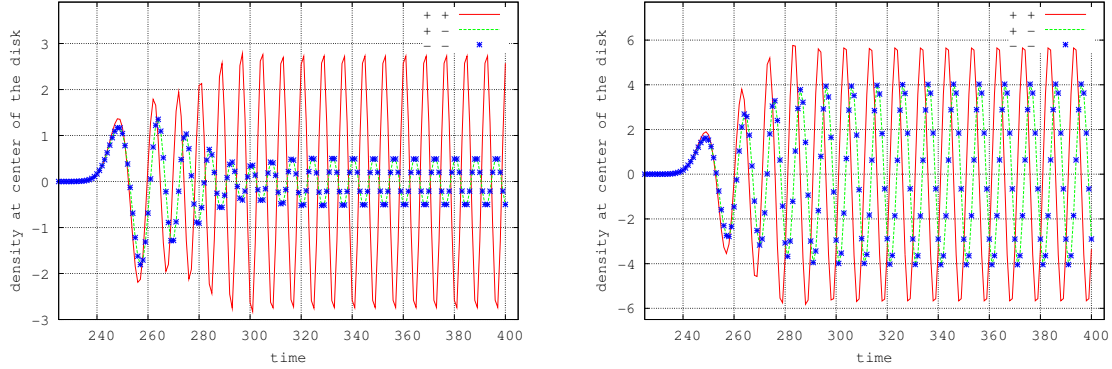


Figure 6. *D2Q13* Converging acoustic propagation, time period = 8 (left) and time period = 10 (right).

6) D3Q27 athermal linearized Acoustics

- The D3Q27 Lattice Boltzmann scheme, described with details *e.g.* in Mei *et al.* [28] is simply obtained by taking a tensorial product for the set \mathcal{V} of discrete velocities:

$$(36) \quad v_j = \lambda (\varepsilon_x, \varepsilon_y, \varepsilon_z), \quad \varepsilon_x, \varepsilon_y, \varepsilon_z = -1, 0, +1, \quad 0 \leq j \leq 26.$$

Due to the large number of moments, we detail in this subsection the way the matrix M parametrizing the transformation (2) is obtained. First, velocities v_j^α for $0 \leq j \leq J \equiv 26$ and $1 \leq \alpha \leq 3$ are given according to relation (36). The first four conserved moments ρ and q^α are determined according to (3). The generation of other moments is done according to the tensorial nature of the variety of moments that can be constructed, as analyzed by Rubinstein and Luo [31]: scalar fields are naturally coupled with one another, *idem* for vector fields, and so on. So components of kinetic energy are introduced:

$$(37) \quad \tilde{m}_4 = e \equiv \sum_{j=0}^{26} \left(\sum_{\beta=1}^3 (v_j^\beta)^2 \right) f_j$$

The entire set of second order tensors is completed according to

$$(38) \quad \left\{ \begin{array}{l} \tilde{m}_5 = XX \equiv \sum_{j=0}^{26} (2(v_j^1)^2 - (v_j^2)^2 - (v_j^3)^2) f_j \\ \tilde{m}_6 = WW \equiv \sum_{j=0}^{26} ((v_j^2)^2 - (v_j^3)^2) f_j \end{array} \right.$$

$$(39) \quad \left\{ \begin{array}{l} \tilde{m}_7 = XY \equiv \sum_{j=0}^{26} v_j^1 v_j^2 f_j \\ \tilde{m}_8 = YZ \equiv \sum_{j=0}^{26} v_j^2 v_j^3 f_j \\ \tilde{m}_9 = ZX \equiv \sum_{j=0}^{26} v_j^3 v_j^1 f_j \end{array} \right.$$

Flux of the energy and of the square of energy:

$$(40) \quad \left\{ \begin{array}{l} \tilde{m}_{9+\alpha} = \varphi_\alpha \equiv 3 \sum_{j=0}^{26} \left(\sum_{\beta=1}^3 (v_j^\beta)^2 \right) v_j^\alpha f_j \\ \tilde{m}_{12+\alpha} = \psi_\alpha \equiv \frac{9}{2} \sum_{j=0}^{26} \left(\sum_{\beta=1}^3 (v_j^\beta)^2 \right)^2 v_j^\alpha f_j, \quad 1 \leq \alpha \leq 3 \end{array} \right.$$

Square and cube of the energy:

$$(41) \quad \left\{ \begin{array}{l} \tilde{m}_{16} = \varepsilon \equiv \frac{3}{2} \sum_{j=0}^{26} \left(\sum_{\beta=1}^3 (v_j^\beta)^2 \right)^2 f_j \\ \tilde{m}_{17} = e_3 \equiv \frac{9}{2} \sum_{j=0}^{26} \left(\sum_{\beta=1}^3 (v_j^\beta)^2 \right)^3 f_j \end{array} \right.$$

Product of XX and WW by the energy:

$$(42) \quad \left\{ \begin{array}{l} \tilde{m}_{18} = XX_e \equiv 3 \sum_{j=0}^{26} (2(v_j^1)^2 - (v_j^2)^2 - (v_j^3)^2) \left(\sum_{\beta=1}^3 (v_j^\beta)^2 \right) f_j \\ \tilde{m}_{19} = WW_e \equiv 3 \sum_{j=0}^{26} ((v_j^2)^2 - (v_j^3)^2) \left(\sum_{\beta=1}^3 (v_j^\beta)^2 \right) f_j \end{array} \right.$$

Extra-diagonal second order moments of the energy: two different components times energy and permutations

$$(43) \quad \left\{ \begin{array}{l} \tilde{m}_{20} = XY_e \equiv 3 \sum_{j=0}^{26} v_j^1 v_j^2 \left(\sum_{\beta=1}^3 (v_j^\beta)^2 \right) f_j \\ \tilde{m}_{21} = YZ_e \equiv 3 \sum_{j=0}^{26} v_j^2 v_j^3 \left(\sum_{\beta=1}^3 (v_j^\beta)^2 \right) f_j \\ \tilde{m}_{22} = ZX_e \equiv 3 \sum_{j=0}^{26} v_j^3 v_j^1 \left(\sum_{\beta=1}^3 (v_j^\beta)^2 \right) f_j \end{array} \right.$$

Third order pseudovector τ_α

$$(44) \quad \tilde{m}_{22+\alpha} = \tau_\alpha \equiv \sum_{j=0}^{26} v_j^\alpha \left((v_j^{\alpha+1})^2 - (v_j^{\alpha-1})^2 \right) f_j, \quad 1 \leq \alpha \leq 3.$$

with a natural permutation convention and the third order totally antisymmetric tensor XYZ :

$$(45) \quad \tilde{m}_{26} = XYZ \equiv \sum_{j=0}^{26} v_j^1 v_j^2 v_j^3 f_j.$$

A first (non-orthogonal) matrix \widetilde{M} is obtained by using (3) (37) (38) (39) (40) (41) (42) (43) (44) and (45) as linear combinations of the f_j 's :

$$(46) \quad \tilde{m}_k \equiv \sum_{j=0}^{26} \widetilde{M}_{kj} f_j, \quad 0 \leq k \leq 26.$$

Then matrix M is orthogonalized from relations (3), (37), (38), (39), (40), (41), (42), (43), (44) and (45) with a Gram-Schmidt orthogonalization algorithm:

$$M_{ij} = \widetilde{M}_{ij} - \sum_{\ell < i} g_{i\ell} M_{\ell j}, \quad i \geq 4.$$

The coefficients $g_{i\ell}$ are computed recursively in order to enforce orthogonality:

$$\sum_{j=0}^{26} M_{ij} M_{kj} = 0 \quad \text{for } i \neq k.$$

Note that the coefficients in (37), (38), (39), (40), (41), (42), (43), (44) and (45) have been chosen such that the coefficients of matrix M are all integers.

- The equilibrium values of the moments define the equilibrium distribution. The first moments ρ and q_α are in equilibrium and have respectively a scalar and a vectorial structure. The equilibrium values of the other moments respect this structure. We have

$$(47) \quad \left\{ \begin{array}{l} e^{\text{eq}} = \theta \lambda^2 \rho \\ XX^{\text{eq}} = WW^{\text{eq}} = XY^{\text{eq}} = YZ^{\text{eq}} = ZX^{\text{eq}} = 0 \\ \varphi_\alpha^{\text{eq}} = c_1 \lambda^2 q_\alpha \\ \psi_\alpha^{\text{eq}} = c_2 \lambda^4 q_\alpha \\ \varepsilon^{\text{eq}} = \beta \lambda^4 \rho \\ e_3^{\text{eq}} = \xi \lambda^6 \rho \\ XX_e^{\text{eq}} = WW_e^{\text{eq}} = XY_e^{\text{eq}} = YZ_e^{\text{eq}} = ZX_e^{\text{eq}} = 0 \\ \tau_\alpha^{\text{eq}} = c_3 \lambda^2 q_\alpha \\ XYZ^{\text{eq}} = 0. \end{array} \right.$$

We have the following relation between the parameter θ and the sound velocity c_0 :

$$(48) \quad \theta = 3c_0^2 - 2.$$

The relaxation parameters for these moments are denoted respectively by the following values

$$(49) \quad \left\{ \begin{array}{ll} e^{\text{eq}} & : s_e \\ XX^{\text{eq}}, WW^{\text{eq}}, XY^{\text{eq}}, YZ^{\text{eq}}, ZX^{\text{eq}} & : s_x \\ \varphi_\alpha^{\text{eq}} & : s_\varphi \\ \psi_\alpha^{\text{eq}} & : s_\psi \\ \varepsilon^{\text{eq}} & : s_\varepsilon \\ e_3^{\text{eq}} & : s_\xi \\ XX_e^{\text{eq}}, WW_e^{\text{eq}} & : s_\gamma \\ XY_e^{\text{eq}}, YZ_e^{\text{eq}}, ZX_e^{\text{eq}} & : s_\chi \\ \tau_\alpha^{\text{eq}} & : s_\tau \\ XYZ^{\text{eq}} & : s_\omega. \end{array} \right.$$

With these relaxation parameters, the shear viscosity is isotropic when

$$(50) \quad \begin{cases} c_1 = -2 \\ c_3 = 0 \end{cases}$$

- The quartic parameters for athermal acoustics are solution of the $13 + 2 + 3 = 18$ discrete equations obtained at Table 2. They are displayed in this subsection.

$$(51) \quad \left\{ \begin{array}{l} \beta = -\frac{1}{2(\sigma_x - \sigma_e)} \left(-9c_0^2\sigma_x - 18c_0^2\sigma_e + 27c_0^4\sigma_x + 180c_0^2\sigma_x\sigma_e^2 \right. \\ \left. + 144c_0^2\sigma_x^3 - 8\sigma_x + 8\sigma_e - 324c_0^4\sigma_x\sigma_e^2 \right) \end{array} \right.$$

$$(52) \quad c_2 = -42\sigma_x^2 + \frac{5}{2}$$

$$(53) \quad \sigma_\varphi = \frac{1}{12\sigma_x}$$

$$(54) \quad \left\{ \begin{array}{l} \sigma_\varepsilon = -\frac{1}{48} \frac{N_\varepsilon}{D_\varepsilon} \\ N_\varepsilon = -76 \sigma_x^2 + 27 c_0^2 - 27 c_0^4 - 180 c_0^2 \sigma_e^2 - 468 c_0^2 \sigma_x^2 + 324 c_0^4 \sigma_e^2 + 7776 c_0^4 \sigma_x^4 \\ \quad - 93312 c_0^4 \sigma_x^4 \sigma_e^2 - 4 \sigma_e^2 + 80 \sigma_x \sigma_e - 336 \sigma_x^3 \sigma_e - 1344 \sigma_e^2 \sigma_x^2 + 240 \sigma_x^4 \\ \quad - 10800 c_0^2 \sigma_x^3 \sigma_e - 46656 c_0^4 \sigma_x^3 \sigma_e^3 + 20736 \sigma_x^3 \sigma_e^3 c_0^2 + 62208 c_0^2 \sigma_x^5 \sigma_e \\ \quad - 324 c_0^4 \sigma_x \sigma_e + 3888 c_0^4 \sigma_x \sigma_e^3 + 864 c_0^2 \sigma_x^2 \sigma_e^2 - 4752 c_0^2 \sigma_x \sigma_e^3 \\ \quad + 51840 c_0^2 \sigma_e^4 \sigma_x^2 + 3888 c_0^4 \sigma_e^2 \sigma_x^2 - 46656 c_0^4 \sigma_e^4 \sigma_x^2 + 324 c_0^2 \sigma_e \sigma_x \\ \quad - 3456 \sigma_x^6 + 2880 \sigma_x^3 \sigma_e^3 + 20736 c_0^2 \sigma_x^6 + 8064 \sigma_x^4 \sigma_e^2 + 6912 \sigma_x^5 \sigma_e \\ \quad - 864 c_0^2 \sigma_x^4 + 1440 \sigma_x \sigma_e^3 - 14400 \sigma_e^4 \sigma_x^2 + 324 c_0^4 \sigma_x^2 + 31104 c_0^2 \sigma_x^4 \sigma_e^2 \\ D_\varepsilon = \sigma_x (\sigma_x - \sigma_e) \left(-84 \sigma_x^3 + 432 c_0^2 \sigma_x^3 + 84 \sigma_x^2 \sigma_e + 540 c_0^2 \sigma_x \sigma_e^2 - 23 \sigma_x \right. \\ \quad \left. - 972 c_0^4 \sigma_x \sigma_e^2 - 27 c_0^2 \sigma_x + 81 c_0^4 \sigma_x + 23 \sigma_e - 54 c_0^2 \sigma_e \right) \end{array} \right.$$

We observe that the presence of the factor $(\sigma_x - \sigma_e)$ in the denominator of the algebraic expression (54) of σ_ε makes this expression incompatible with a BGK or TRT [15] type hypothesis. The same remark holds for relations (55) and (56) relative to the parameters σ_γ and σ_χ respectively.

$$(55) \quad \left\{ \begin{array}{l} \sigma_\gamma = \frac{1}{336 \sigma_x (-1 + 12 \sigma_x^2) (\sigma_x - \sigma_e)^2} N_\gamma \\ N_\gamma = 1968 \sigma_x^4 - 144 c_0^2 \sigma_x^2 - 15552 c_0^2 \sigma_x^4 - 624 \sigma_e^2 \sigma_x^2 - 1344 \sigma_x^3 \sigma_e \\ \quad + 4608 \sigma_x^5 \sigma_e + 8064 \sigma_x^4 \sigma_e^2 - 12672 \sigma_x^6 + 103680 c_0^2 \sigma_x^4 \sigma_e^2 \\ \quad - 186624 c_0^4 \sigma_x^4 \sigma_e^2 - 27 c_0^4 + 27 c_0^2 - 4 \sigma_e^2 + 324 c_0^4 \sigma_e^2 - 180 c_0^2 \sigma_e^2 \\ \quad + 80 \sigma_x \sigma_e - 76 \sigma_x^2 + 82944 c_0^2 \sigma_x^6 + 15552 c_0^4 \sigma_x^4 \end{array} \right.$$

$$(56) \quad \left\{ \begin{array}{l} \sigma_\chi = \frac{1}{96 \sigma_x (-1 + 84 \sigma_x^2) (\sigma_x - \sigma_e)^2} N_\chi \\ N_\chi = 192 \sigma_x^4 - 828 c_0^2 \sigma_x^2 + 972 c_0^4 \sigma_x^2 + 6480 c_0^2 \sigma_x^2 \sigma_e^2 - 2592 c_0^2 \sigma_x^4 \\ \quad - 11664 c_0^4 \sigma_e^2 \sigma_x^2 + 192 \sigma_e^2 \sigma_x^2 - 384 \sigma_x^3 \sigma_e + 2304 \sigma_x^5 \sigma_e + 4032 \sigma_x^4 \sigma_e^2 \\ \quad - 6336 \sigma_x^6 + 76 \sigma_x^2 + 51840 c_0^2 \sigma_x^4 \sigma_e^2 - 93312 c_0^4 \sigma_x^4 \sigma_e^2 + 27 c_0^4 - 27 c_0^2 \\ \quad + 4 \sigma_e^2 - 324 c_0^4 \sigma_e^2 + 180 c_0^2 \sigma_e^2 - 80 \sigma_x \sigma_e + 41472 c_0^2 \sigma_x^6 + 7776 c_0^4 \sigma_x^4 \end{array} \right.$$

$$(57) \quad \left\{ \begin{array}{l} \sigma_\tau = \frac{1}{12} \frac{N_\tau}{D_\tau} \\ N_\tau = 76 \sigma_x^2 - 324 c_0^4 \sigma_e^2 + 180 c_0^2 \sigma_e^2 - 144 \sigma_x^4 - 80 \sigma_x \sigma_e + 3456 c_0^2 \sigma_x^4 \\ \quad + 720 \sigma_e^2 \sigma_x^2 - 576 \sigma_x^3 \sigma_e - 504 c_0^2 \sigma_x^2 + 4320 c_0^2 \sigma_x^2 \sigma_e^2 + 27 c_0^4 + 4 \sigma_e^2 \\ \quad - 27 c_0^2 - 7776 c_0^4 \sigma_e^2 \sigma_x^2 + 648 c_0^4 \sigma_x^2 \\ D_\tau = \sigma_x (76 \sigma_x^2 - 528 \sigma_x^4 - 504 c_0^2 \sigma_x^2 + 648 c_0^4 \sigma_x^2 + 4320 c_0^2 \sigma_x^2 \sigma_e^2 \\ \quad + 3456 c_0^2 \sigma_x^4 - 7776 c_0^4 \sigma_e^2 \sigma_x^2 + 336 \sigma_e^2 \sigma_x^2 + 192 \sigma_x^3 \sigma_e + 27 c_0^4 - 27 c_0^2 \\ \quad + 4 \sigma_e^2 - 324 c_0^4 \sigma_e^2 + 180 c_0^2 \sigma_e^2 - 80 \sigma_x \sigma_e) \end{array} \right.$$

$$(58) \quad \left\{ \begin{array}{l} \sigma_\omega = \frac{1}{12} \frac{N_\omega}{D_\omega} \\ N_\omega = -816 \sigma_x^4 - 828 c_0^2 \sigma_x^2 + 972 c_0^4 \sigma_x^2 + 6480 c_0^2 \sigma_x^2 \sigma_e^2 - 2592 c_0^2 \sigma_x^4 \\ \quad - 11664 c_0^4 \sigma_e^2 \sigma_x^2 - 816 \sigma_e^2 \sigma_x^2 + 1632 \sigma_x^3 \sigma_e - 17280 \sigma_x^5 \sigma_e + 13824 \sigma_x^4 \sigma_e^2 \\ \quad + 3456 \sigma_x^6 + 76 \sigma_x^2 + 51840 c_0^2 \sigma_x^4 \sigma_e^2 - 93312 c_0^4 \sigma_x^4 \sigma_e^2 + 27 c_0^4 - 27 c_0^2 \\ \quad + 4 \sigma_e^2 - 324 c_0^4 \sigma_e^2 + 180 c_0^2 \sigma_e^2 - 80 \sigma_x \sigma_e + 41472 c_0^2 \sigma_x^6 + 7776 c_0^4 \sigma_x^4 \\ D_\omega = \sigma_x \left(-192 \sigma_x^4 - 828 c_0^2 \sigma_x^2 + 972 c_0^4 \sigma_x^2 + 6480 c_0^2 \sigma_x^2 \sigma_e^2 - 2592 c_0^2 \sigma_x^4 \right. \\ \quad - 11664 c_0^4 \sigma_e^2 \sigma_x^2 - 192 \sigma_e^2 \sigma_x^2 + 384 \sigma_x^3 \sigma_e + 2304 \sigma_x^5 \sigma_e + 4032 \sigma_x^4 \sigma_e^2 \\ \quad - 6336 \sigma_x^6 + 76 \sigma_x^2 + 51840 c_0^2 \sigma_x^4 \sigma_e^2 - 93312 c_0^4 \sigma_x^4 \sigma_e^2 + 27 c_0^4 - 27 c_0^2 \\ \quad \left. + 4 \sigma_e^2 - 324 c_0^4 \sigma_e^2 + 180 c_0^2 \sigma_e^2 - 80 \sigma_x \sigma_e + 41472 c_0^2 \sigma_x^6 + 7776 c_0^4 \sigma_x^4 \right) \end{array} \right.$$

For the numerical experiments described above, we have used the following values of the equilibrium parameters. We did the previous theoretical numerical computations (51) (52) (53) (54) (55) (56) (57) (58) with a 50 Digits option in our symbolic manipulation software:

$$(59) \quad \left\{ \begin{array}{l} s_e = 0.95057034220532319391634980988593155893536121673004 \\ s_x = 1.8552875695732838589981447124304267161410018552876 \\ c_0 = 0.623538 \\ c_2 = 2.436118000 \\ \xi = 1 \end{array} \right.$$

and the ‘‘quartic’’ relaxation parameters:

$$(60) \quad \left\{ \begin{array}{l} \beta = 0.50345521670787922851706691010021052631578947368420 \\ s_\phi = 0.37925445705024311183144246353322528363047001620745 \\ s_\psi = 1.3 \\ s_\varepsilon = 0.34253657030513141274711235609982461596733955718034 \\ s_\xi = 1.2 \\ s_\gamma = 1.9945477114942149093456286590460711496091258797386 \\ s_\chi = 1.2940799466197218037166471960307116873345869400515 \\ s_\tau = 1.9451616927239606019667013153498030552793202566039 \\ s_\omega = 0.25131560984615404581501005329813711811837082814760. \end{array} \right.$$

Of course, we used the previous numbers with the usual truncation allowed by the 32 bit or 64 bit floating point arithmetic. We observe that for these particular parameters, due to the link (33) between the shear viscosity μ and the parameter σ_x , to relation (34) between the bulk viscosity ζ and the parameter σ_e and to formula (28) making explicit the attenuation γ of sound waves, we have

$$(61) \quad \left\{ \begin{array}{l} \mu = 0.013 \lambda \Delta x \\ \zeta = 0.0920492 \lambda \Delta x \\ \gamma = 0.0546913 \lambda \Delta x. \end{array} \right.$$

- The results of simple periodic waves are displayed in Figures 7, 8 and 9. The numerical results confirm that parameters proposed in (59) and (60) allow one to get fourth order (relative) accuracy.

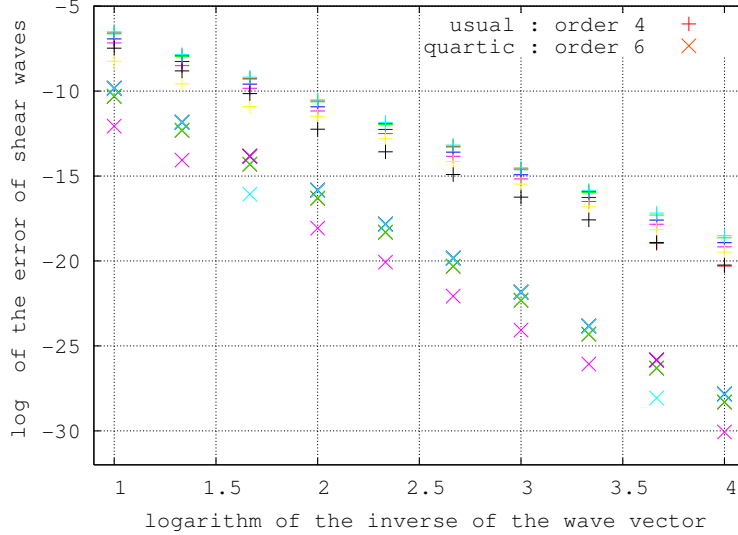


Figure 7. Periodic wave with the lattice Boltzmann scheme $D3Q27$. Error for shear eigenvalue Γ_t defined in (32). For quartic parameters, we have $\Gamma_t - \nu |\mathbf{k}|^2 = O(|\mathbf{k}|^6)$.

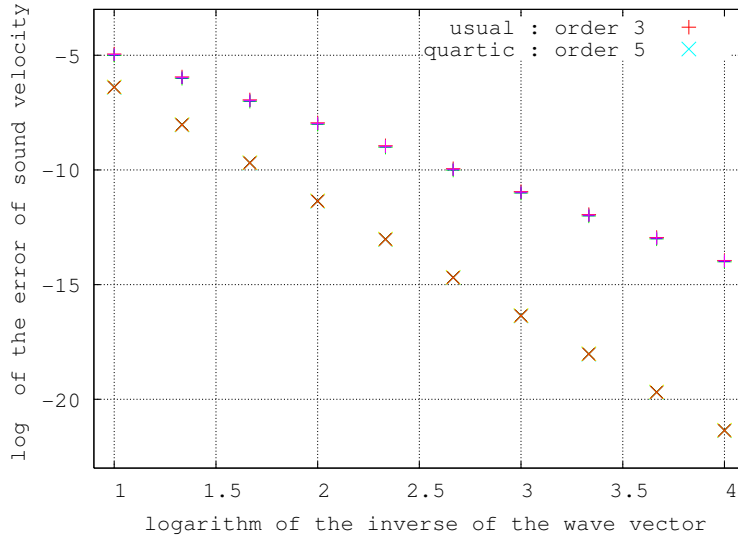


Figure 8. Periodic wave with the lattice Boltzmann scheme $D3Q27$. Error for the imaginary part of the acoustic eigenvalue Γ_ℓ defined in (30). For quartic parameters, we have fifth order accuracy: $\text{Im}(\Gamma_\ell) - c_0 |\mathbf{k}| (1 - \gamma^2 |\mathbf{k}|^2 / (2 c_0^2)) = O(|\mathbf{k}|^5)$ with γ detailed at relation (28).

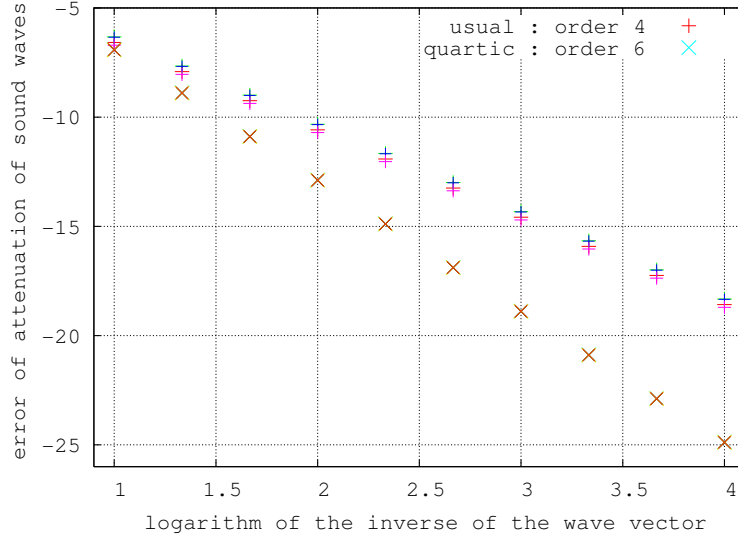


Figure 9. Periodic wave with the lattice Boltzmann scheme D3Q27. Error for the real part of acoustic eigenvalue Γ_ℓ . For quartic parameters, we have $\text{Re}(\Gamma_\ell) - \gamma |\mathbf{k}|^2 = O(|\mathbf{k}|^6)$.

The numerical experiments have been done for a three-dimensional converging acoustic wave. A pulsating sphere of radius $R = 46.08$ is embedded in a 95^3 cube. The simulations used only 64 bit or even 32 bit data with CUDA: (using a Nvidia 9800GT card, one full update of D3Q27 takes approximately 11 nanoseconds per site). The “linear anti-bounce-back” numerical boundary conditions (in the sense given in Bouzidi *et al.* [1]) are used to impose a boundary density on the sphere oscillating with a period $T = 10$. Since the sound velocity is around 0.62 (see (59)), there are around six mesh points by wave length. In Figure 10, the scatter plot of density *vs* radius after 82 iterations is displayed. The results are of excellent quality with the use of quartic parameters. Nevertheless, since the attenuation of the sound wave is relatively important for the above parameters ($\gamma \approx 0.0547$ as recalled in (61)), the range of propagation is relatively limited (five wave lengths in our case, see Figure 10). For the less stringent “isotropic” case, *i.e.* to fix the ideas

$$(62) \quad \begin{cases} \sigma_\phi = \frac{1}{6\sigma_x} \\ \beta = 4 - 9c_0^2 \\ c_0 = \frac{1}{\sqrt{3}} \end{cases}$$

we can find situations of “TRT type” satisfying

$$(63) \quad \begin{cases} \sigma_\phi = \sigma_\psi = \sigma_\tau = \sigma_\omega \\ \sigma_e = \sigma_x = \sigma_\epsilon = \sigma_\xi = \sigma_\gamma = \sigma_\chi \end{cases}$$

with much lower attenuation of sound. An example is given in figure 10 with parameters of the scheme following relations (62) and (63) with $\sigma_x = 0.006$, that is shear viscosity 0.002 and sound attenuation 0.002. These results show that choosing the goal in terms of accuracy or small attenuation will influence the choice of the parameters in the lattice Boltzmann simulation.

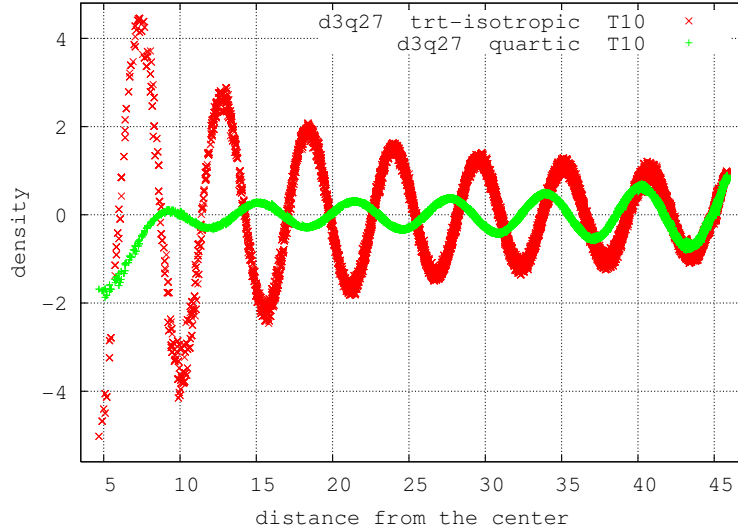


Figure 10. *Sound wave emitted by a sphere. Numerical results with the D3Q27 lattice Boltzmann scheme with “TRT” isotropic parameters described at relations (62) (63) and with quartic parameters given by relations (59) and (60). Six points by wave length.*

7) Conclusion

- We have proposed to use the Taylor expansion method in conjunction with the use of symbolic manipulation to increase the accuracy of the lattice Boltzmann scheme in the multiple time relaxation approach proposed by D. d’Humières for linear acoustic waves. The result is the use of the previous scheme with very particular “quartic” parameters. We have obtained a family of such parameters for the D3Q27 numerical scheme. Numerical experiments confirm the predictions of the theoretical analysis. The catch is to make sure that situations are stable. This problem cannot be solved in practice with developments around small wave numbers. In the absence of efficient techniques to find stable situations with small viscosities and/or sound attenuation, we tried at random a number of sets of the free parameters and have used the best of them for the explicit results shown above. We note that the less stringent “isotropic” condition is compatible with small viscosities which may be quite useful for practical simulations. Comparison of various stencils is under way and will be presented elsewhere.

Acknowledgments

The referees conveyed to the authors very interesting remarks. Some of them have been incorporated into the present edition of the article.

References

- [1] M. Bouzidi, M. Firdaouss and P. Lallemand. “Momentum transfer of a Boltzmann lattice fluid with boundaries”, *Physics of Fluids*, vol. **13**, n° 11, p. 3452-3459, 2001.
- [2] R. Carpentier, A. de La Bourdonnaye, B. Larrouturou. “On the derivation of the modified equation for the analysis of linear numerical methods”, *RAIRO - Modélisation mathématique et analyse numérique*, vol. **31**, p. 459-470, 1997.
- [3] C. Cohen-Tannoudji, B. Diu , F. Laloë. *Quantum Mechanics*, two volumes, Wiley , 1978.
- [4] Y. Chen, H. Ohashi, M. Akiyama. “Thermal lattice Bhatnagar-Gross-Krook model without nonlinear deviations in macrodynamic equations”, *Physical Review E*, vol. **50**, p. 2776-2783, 1994.
- [5] D. d’Humières. “Generalized Lattice-Boltzmann Equations”, in *Rarefied Gas Dynamics: Theory and Simulations*, vol. **159** of *AIAA Progress in Astronautics and Astronautics*, p. 450-458, 1992.
- [6] D. d’Humières, P. Lallemand and U. Frisch. “Lattice gas models for 3D–hydrodynamics”, *Europhysics Letters*, vol. **2**, n° 4, p. 291-297, 1986.
- [7] P. J. Dellar. “Lattice kinetic schemes for magnetohydrodynamics”, *Journal of Computational Physics*, vol. **179**, p. 95-126, 2002.
- [8] F. Dubois. “Une introduction au schéma de Boltzmann sur réseau”, *ESAIM: Proceedings*, vol. **18**, p. 181-215, 2007.
- [9] F. Dubois. “Equivalent partial differential equations of a lattice Boltzmann scheme”, *Computers and mathematics with applications*, vol. **55**, p. 1441-1449, 2008.
- [10] F. Dubois. “Third order equivalent equation of lattice Boltzmann scheme”, *Discrete and Continuous Dynamical Systems*, vol. **23**, numbers 1 & 2, p. 221-248, January and February 2009.
- [11] F. Dubois, P. Lallemand. “Towards higher order lattice Boltzmann schemes”, *Journal of Statistical Mechanics: Theory and Experiment*, P06006 doi: 10.1088/1742-5468/2009/06/P06006, 2009.

- [12] F. Dubois, P. Lallemand, M. Tekitek. “On a superconvergent lattice Boltzmann boundary scheme”, *Computers and Mathematics with Applications*, vol. **59**, p. 2141-2149, doi:10.1016/j.camwa.2009.08.055, 2010.
- [13] M. Geier, A. Greiner and J.G. Korvink. “Cascaded digital lattice Boltzmann automata for high Reynolds number flow”, *Physical Review E*, vol. **73**, p. 066705, 2006.
- [14] I. Ginzburg, P.M. Adler. “Boundary flow condition analysis for three-dimensional lattice Boltzmann model”, *Journal of Physics II France*, vol. **4**, p. 191-214, 1994.
- [15] I. Ginzburg, F. Verhaeghe and D. d’Humières. “Study of Simple Hydrodynamic Solutions with the Two-Relaxation-Times Lattice Boltzmann Scheme”, *Communications in Computational Physics*, vol. **3**, p. 519-581, 2008.
- [16] D. Griffiths, J. Sanz-Serna. “On the scope of the method of modified equations”, *SIAM Journal on Scientific and Statistical Computing*, vol. **7**, p. 994-1008, 1986.
- [17] J. Hardy, Y. Pomeau and O. de Pazzis. “Time Evolution of a Two-Dimensional Classical Lattice System”, *Physical Review Letters*, vol. **31**, p. 276 - 279, 1973.
- [18] M. Hénon. “Viscosity of a Lattice Gas”, *Complex Systems*, vol. **1**, p. 763-789, 1987.
- [19] E.J. Hinch. *Perturbation methods*, Cambridge University Press, 1991.
- [20] F. Higuera, S. Succi and R. Benzi. “Lattice gas dynamics with enhanced collisions”, *Europhysics Letters*, vol. **9**, n° 4, p. 345-349, 1989.
- [21] L. Hörmander. *The Analysis of Linear Partial Differential Operators III: Pseudo-Differential Operators*, Springer-Verlag, Berlin, Heidelberg, 1985.
- [22] Y.W. Kwon. “Coupling of Lattice Boltzmann and Finite Element Methods for Fluid-Structure Interaction Application”, *Journal of Pressure Vessel Technology*, vol. **130**, n° 1, 011302 (6 pages), doi:10.1115/1.2826405, 2008.
- [23] P. Lallemand, L.-S. Luo. “Theory of the lattice Boltzmann method: Dispersion, dissipation, isotropy, Galilean invariance, and stability”, *Physical Review E*, vol. **61**, p. 6546-6562, June 2000.
- [24] L.D. Landau, E.M. Lifshitz. *Fluid Mechanics*, Pergamon Press, London, 1959.
- [25] A. Lerat, R. Peyret. “Noncentered Schemes and Shock Propagation Problems”, *Computers and Fluids*, vol. **2**, p. 35-52, 1974.

- [26] E. Leriche, P. Lallemand and G. Labrosse. “Stokes eigenmodes in cubic domain: primitive variable and Lattice Boltzmann formulations”, *Applied Numerical Mathematics*, vol. **58**, p. 935-945, 2008.
- [27] G. Mc Namara, G. Zanetti. “Use of Boltzmann equation to simulate lattice gas automata”, *Physical Review Letters*, vol. **61**, n° 20, p. 2332-2335, 1988.
- [28] R. Mei, W. Shyy, D. Yu, L.S. Luo. “Lattice Boltzmann method for 3-D flows with curved boundary”, *Journal of Computational Physics*, vol. **161**, p. 680-699, 2000.
- [29] Y.H. Qian, D. d’Humières and P. Lallemand. “Lattice BGK for Navier–Stokes equation”, *Europhysics Letters*, vol. **17**, n° 6, p. 479-484, 1992.
- [30] Y.H. Qian. “Simulating thermohydrodynamics with lattice BGK models”, *Journal of Scientific Computing*, vol. **8**, p. 231-242, 1993.
- [31] R. Rubinstein, L.-S. Luo. “Theory of the lattice Boltzmann equation: Symmetry properties of discrete velocity sets”, *Physical Review E (Statistical, Nonlinear, and Soft Matter Physics)*, vol. **77**:036709, 2008.
- [32] J. Tölke, M. Krafczyk, M. Schulz and E. Rank. “Lattice Boltzmann Simulations of Binary Fluid Flow through Porous Media”, *Philosophical Transactions of the Royal Society A.*, London, vol. **360**, p. 535-545, 2002.
- [33] F.R. Villatoro, J.I. Ramos. “On the method of modified equations. V: Asymptotic analysis of and direct-correction and asymptotic successive-correction techniques for the implicit midpoint method”, *Applied Mathematics and Computation*, **103**, p. 241-285, 1999.
- [34] R.F. Warming, B.J. Hyett. “The modified equation approach to the stability and accuracy analysis of finite difference methods”, *Journal of Computational Physics*, vol. **14**, p. 159-179, 1975.
- [35] J.R. Weimar, J.P. Boon. “Nonlinear reactions advected by a flow”, *Physica A*, vol. **224**, p. 207-215, 1996.
- [36] S. Wolfram. “Cellular Automaton fluids: basic theory”, *Journal of Statistical Physics*, vol. **45**, p. 471-526, 1986.